Available online at www.sciencedirect.com

ScienceDirect

International Journal of Thermal Sciences 46 (2007) 245–252

International Journal of Thermal Sciences

www.elsevier.com/locate/ijts

Constructal multi-scale design of compact micro-tube heat sinks and heat exchangers

Y.S. Muzychka

Faculty of Engineering and Applied Science, Memorial University of Newfoundland, St. John's, NF, Canada A1B 3X5

Received 30 August 2005; received in revised form 30 January 2006; accepted 11 May 2006

Available online 11 July 2006

Abstract

A constructal multi-scale design approach is examined for micro-tube heat sinks and heat exchangers. Heat transfer per unit volume is increased by considering the use of additional micro-tubes placed in the intersticial regions of a circular tube array. Three constructs are considered in the proposed analysis. As the system complexity increases, the heat transfer rate increases, and exceeds the theoretical value for a volume of similar size, composed of parallel plates. Approximate solutions for the diameter of the principal construct are obtained for each case using Bejan's intersection of asymptotes method. Exact analytical methods are applied to determine the relative increase in heat dissipation per unit volume as compared with systems containing parallel plates.

Keywords: Constructal design; Heat sinks; Heat exchangers; High heat flux; Forced convection; Laminar flow

1. Introduction

Micro-tube and micro-channel cooling devices are becoming more prevalent in engineering systems. High heat flux applications require solutions which minimize the overall package thermal resistance, or in other words, maximize heat transfer per unit volume. In space constrained applications, such as micro-chip cooling, micro-tube technology is finding widespread application, since large numbers of these tubes may be accommodated in a small space. Efficient thermal design requires that the diameter of these tubes be optimal for a prescribed set of flow conditions. The idea of a *designed porous media* was recently put forth by Bejan [1], and is discussed further in the recent text by Bejan et al. [2]. In this design philosophy, thermal optimization within a fixed volume leads to a flow architecture which is essentially a complex porous structure, which has been designed for minimum thermal resistance.

Several approaches exist for choosing this optimal duct diameter. These include classical optimization techniques such as the direct search method or the Lagrange multiplier method; or simpler modern techniques such as the intersection of asymptotes method, proposed by Bejan [3,4]. Recently, the author [5] applied Bejan's intersection of asymptotes method for geometries widely used in compact heat exchangers, and obtained the optimal dimensions for arrays of circular and non-circular ducts. In the present work, a constructal multi-scale design approach is presented which allows for maximum heat dissipation in systems utilizing circular micro-tubes. Multi-scale design utilizes multiple length scales to assist in maximizing heat transfer density or effectively minimizing the global thermal resistance of the system of interest. Recently, Bejan and Fautrelle [6] demonstrated the methodology for a system composed of parallel plates. By means of inserting additional plates in the under utilized regions of the flow, the heat transfer density of the structure was increased. Bello-Ochende and Bejan [7] further studied this system using numerical methods.

The circular tube is an optimal construction in nature, and hence is also most frequently used in engineering design. However, due to the fact that circular tubes do not allow for efficient packing as compared with parallel plates, square ducts, or triangular ducts, maximum heat dissipation rates tend to be lower in systems composed of tubes as shown in Table 1. These solu-

E-mail address: yuri@engr.mun.ca (Y.S. Muzychka).

1290-0729/$ – see front matter © 2006 Elsevier Masson SAS. All rights reserved.
doi:10.1016/j.ijthermalsci.2006.05.002

Nomenclature

A	flow area	m^2
Be	Bejan number, $\equiv \Delta p L^2/\mu\alpha$	
C_1	constant	
C_p	specific heat	$J\,kg^{-1}\,K^{-1}$
d	diameter of circular duct	m
e	effectiveness	
f	friction factor, $\equiv \tau/(\frac{1}{2}\rho U^2)$	
$f\,Re_{\mathcal{L}}$	friction factor Reynolds number, $\equiv 2\bar{\tau}\mathcal{L}/\mu\overline{U}$	
k	thermal conductivity	$W\,m^{-1}\,K^{-1}$
$\bar{h}$	heat transfer coefficient	$W\,m^{-2}\,K^{-1}$
H	height	m
L	duct length	m
$\dot{m}$	mass flow rate	$kg\,s^{-1}$
n	constructal level	
N	number of ducts	
NTU	number of transfer units	
P	perimeter	m
p	pressure	$N\,m^{-2}$
Pr	Prandtl number, $\equiv \nu/\alpha$	
Q	heat transfer rate	W
$\mathcal{Q}$	heat transfer per unit volume, $\equiv Q/HWL$	
$Q^\star$	dimensionless $\mathcal{Q}$, $\equiv \mathcal{Q}L^2/k(\overline{T}_s - T_i)$	
$Re_{\mathcal{L}}$	Reynolds number, $\equiv U\mathcal{L}/\nu$	
$\overline{T}_s$	wall or surface temperature	K
T_i	fluid inlet temperature	K
$\overline{U}$	average velocity	$m\,s^{-1}$
U_∞	free stream velocity	$m\,s^{-1}$
W	width	m
z^+	dimensionless hydrodynamic duct length, $\equiv L/\mathcal{L}Re_{\mathcal{L}}$	
z^*	dimensionless thermal duct length, $\equiv L/\mathcal{L}Re_{\mathcal{L}}Pr$	

Greek symbols

α	thermal diffusivity	$m^2\,s^{-1}$
δ_1	dimensionless optimal diameter, $\equiv \frac{d_1}{L}Be^{1/4}$	
μ	dynamic viscosity	$N\,s\,m^{-2}$
ν	kinematic viscosity	$m^2\,s^{-1}$
ρ	fluid density	$kg\,m^{-3}$
τ	wall shear stress	$N\,m^{-2}$

Subscripts

a	approximate
app	apparent
e	exact
f	fluid
i	construct
l	large
$\mathcal{L}$	based upon the arbitrary length $\mathcal{L}$
opt	optimum
s	small
w	wall

Table 1
Exact solutions for parallel plates and circular tubes versus Prandtl number

Pr	$(b_{opt}/L)Be^{1/4}$	$Q^\star/Be^{1/2}$
Parallel plates [8]		
0.72	3.033	0.479
6	3.077	0.522
20	3.078	0.527
100	3.055	0.526
1000	3.025	0.523
Circular tubes [9]		
0.1	5.261	0.2348
1	4.971	0.3369
10	5.234	0.3783
100	5.284	0.3843

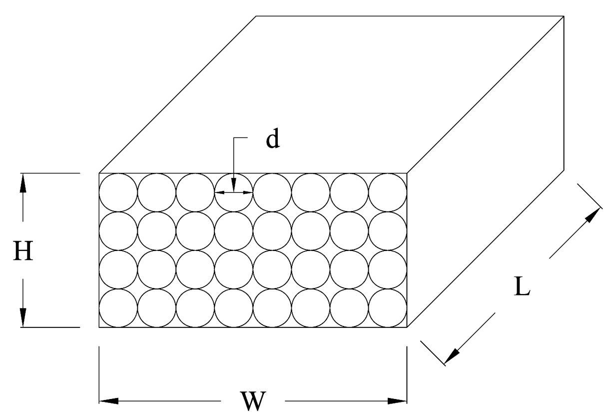

Fig. 1. Compact tube heat sink/heat exchanger [5].

tions are from the work of Bejan and Sciubba [8] and Yilmaz et al. [9] who examined finite volumes of parallel plates and circular tubes. This issue can be alleviated through the use of multi-scale design. In a fixed volume, a finite number of equal diameter tubes may be aligned in a square packing arrangement, as shown in Fig. 1, or some other known distribution. The principle behind the constructal multi-scale approach, is to pack additional tubes of smaller diameter in the interstitial regions which represent under utilized space for cooling ducts, as shown in Fig. 2. Ideally, in such a system, there would be material around each tube as shown, but in the foregoing analysis it is assumed that the largest number of tubes occurs when all tubes are in contact. This also leads to simple recursive relationships for the tube layouts under consideration. Three constructs will be considered. These are the principal construct as found in Muzychka [5], which is based on the simple square packing arrangement, a secondary construct, and a tertiary construct. With the addition of each new construct, it will be shown that the theoretical heat transfer rate per unit volume increases. In other words as the complexity of the structure increases, the overall thermal resistance decreases.

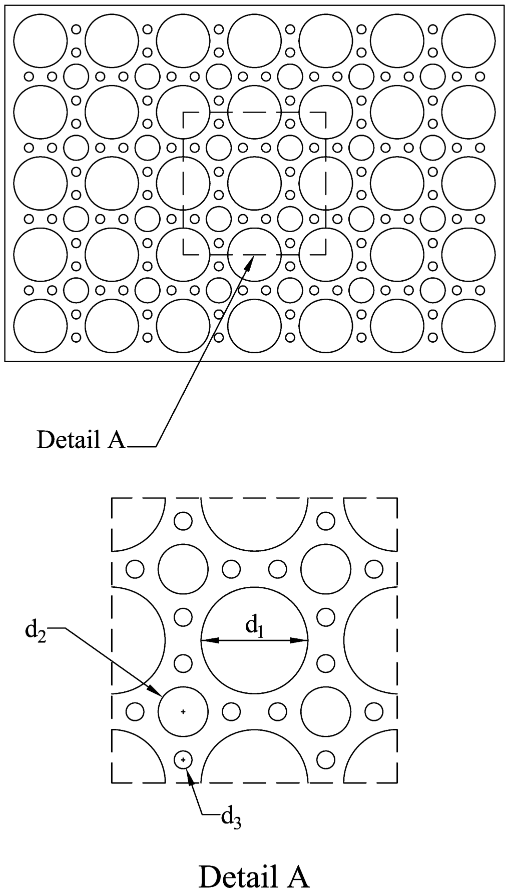

Fig. 2. Multi-scale design of micro-tube heat transfer device.

2. General theory

The basic theory for the multi-scale structure will now be developed. The structure will be assumed to be composed of multiple diameter tubes of a particular arrangement. Further, the structure will be assumed to be composed of a highly conductive material which results in nearly isothermal walls. Finally, laminar flow is assumed to prevail through out the structure. The basic theory will be developed for the most general case of an array of circular tubes containing n numbers of tubes of diameter d_i, for $i = 1, \dots, n$. Later a specific case of circular tubes arranged on square centers with interstitial tubes will be considered.

2.1. Small duct diameter

In the case of an array of ducts with multiple small cross-sectional characteristic reference length scales, the enthalpy balance for fully developed flow gives:

$$Q_s = \sum_{i=1}^{n} \rho \overline{U}_i N_i A_i C_p \Delta T \tag{1}$$

where A_i is the cross-sectional area of an elemental duct, N_i is the number of such ducts, and $\Delta T = \overline{T}_s - T_i$ is the surface to inlet temperature difference.

The mean velocity, $\overline{U}_i$, in any one duct assuming uniform flow, may be determined from the fully developed flow Poiseuille number defined as:

$$\frac{f\,Re_d}{2} = \frac{\bar{\tau}_w d_i}{\mu \overline{U}_i} = \frac{(A_i/P_i)(\Delta p/L) d_i}{\mu \overline{U}_i} = 8 \tag{2}$$

or

$$\overline{U}_i = \frac{\Delta p d_i^2}{32 \mu L} \tag{3}$$

Combining Eqs. (1) and (3) gives the heat transfer rate in terms of the fundamental flow quantities:

$$Q_s = \frac{\pi \rho \Delta p C_p \Delta T}{128 \mu L} \sum_{i=1}^{n} N_i d_i^4 \tag{4}$$

for a collection of various sized tubes. The value of N_i for a given array must be determined for the cross-section, HW, in terms of a characteristic dimensions of the ducts in the array and the layout. By means of simple recursive relationships, three levels of flow architecture may be considered, and the overall energy balance written in terms of the principal tube diameter.

2.2. Large duct diameter

In the case of an array of ducts with large cross-sectional characteristic length scales, the heat transfer rate may be adequately approximated as boundary layer flow in this limit, Muzychka and Yovanovich [10]. The heat transfer rate is determined from:

$$Q_l = \sum_{i=1}^{n} \bar{h} P_i L \Delta T \tag{5}$$

where $\bar{h}$ may be defined from the expression for laminar boundary layer flow over a flat plate:

$$\frac{\bar{h} L}{k_f} = 0.664 \left(\frac{U_\infty L}{\nu} \right)^{1/2} Pr^{1/3} \tag{6}$$

The free stream velocity U_∞, is obtained from a force balance on the array:

$$\bar{\tau}_w \sum_{i=1}^{n} P_i L N_i = \Delta p \sum_{i=1}^{n} N_i A_i \tag{7}$$

where the mean wall shear stress is obtained from the boundary layer solution:

$$\frac{\bar{\tau}_w}{\frac{1}{2} \rho U_\infty^2} = 1.328 \left(\frac{U_\infty L}{\nu} \right)^{-1/2} \tag{8}$$

Combining Eqs. (7) and (8) yields the following result for U_∞:

$$U_\infty = 1.314 \left(\frac{\Delta p \sum_{i=1}^{n} N_i d_i^2}{4 \rho \sqrt{\nu} \sqrt{L} \sum_{i=1}^{n} N_i d_i} \right)^{2/3} \tag{9}$$

Finally, combining Eqs. (5), (6) and (9) yields the following result for the heat transfer rate:

$$Q_l = 1.506 k_f \Delta T \left(\frac{Pr \Delta p L}{\rho \nu^2}\right)^{1/3} \sum_{i=1}^{n} \left(\frac{\sum_{i=1}^{n} N_i d_i^2}{\sum_{i=1}^{n} N_i d_i}\right)^{1/3} N_i d_i \tag{10}$$

Once again, we see that the heat transfer rate is directly proportional to the number of ducts in the array structure.

2.3. Optimal duct size

The optimal duct or channel size may be found by means of the method of intersecting asymptotes [3,4]. The exact shape of the heat transfer rate curve may be found using more exact methods such as expressions found in Shah and Sekulic [11] or Muzychka and Yovanovich [10]. However, the intersection point of the two asymptotic results is relatively close to the exact point as shown in Fig. 3. In this way, an approximate value for the duct dimensions may be found. Intersecting Eqs. (4) and (10) gives:

$$61.35\left(\frac{\alpha^2 \mu^2 L^4}{\Delta p^2}\right)^{1/3} \approx \frac{\sum_{i=1}^{n} N_i d_i^4}{\sum_{i=1}^{n} (\sum_{i=1}^{n} N_i d_i^2 / \sum_{i=1}^{n} N_i d_i)^{1/3} N_i d_i} \tag{11}$$

after collecting and simplifying. We may write the above equation in terms of the Bejan number, as:

$$61.35 \frac{L^{8/3}}{Be^{2/3}} \approx \frac{\sum_{i=1}^{n} N_i d_i^4}{\sum_{i=1}^{n} (\sum_{i=1}^{n} N_i d_i^2 / \sum_{i=1}^{n} N_i d_i)^{1/3} N_i d_i} \tag{12}$$

where $Be = \Delta p L^2 / \mu\alpha$. The left-hand side is determined by the system constraints of flow length, pressure drop, and working fluid, while the right-hand side determines the optimal tube diameters. Once a system architecture is proposed, that is the number of constructs, and the relationship between constructs is known, Eq. (12) may be solved for the principal duct diameter, from which all others follow.

2.4. Maximum heat transfer density

The maximum heat transfer rate for a fixed volume can be obtained from Eq. (4) or (10) using the optimal result determined by Eq. (12). The number of ducts N_i, which appears in the final result may then be cast in terms of the cooling volume cross-section HW and the principal duct diameter. In this way, the maximum heat transfer per unit volume may be determined. Subsequent results may then be presented in terms of the following dimensionless heat transfer per unit volume:

$$Q^\star \lesssim \frac{\mathcal{Q} L^2}{k(\overline{T}_s - T_i)} = C_1 Be^{1/2} \tag{13}$$

where $\mathcal{Q} = Q/(HWL)$ is the heat transfer per unit volume, and C_1 is a numerical constant determined from the system geometry.

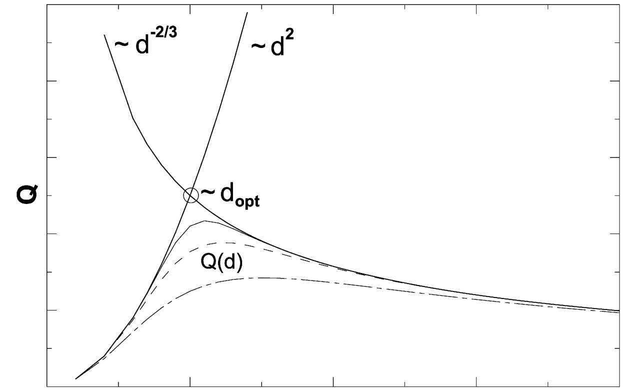

Fig. 3. Method of intersecting asymptotes.

3. Constructal approach

The constructal approach [3,4] is based on the principle of maximization of flow access. Further, through the use of the intersection of asymptotes method, simple solutions for the optimal tube diameters can be easily derived for various configurations. These simple solutions may then be used to develop approximate solutions for the maximum heat transfer density, or they may be used to determine the maximum heat transfer density with greater accuracy by first computing the necessary transport coefficients and then using the appropriate heat exchanger model. This hybrid approach has the advantage of yielding more accurate results with only a marginal increase in effort.

In the present analysis three constructs are considered. These are illustrated in Fig. 4, which illustrates the basic cell for each case. It can be shown that the second and third constructs may be related to the first or principal construct when the ducts are in contact with each other as shown. The following relationships are derived through simple geometric analysis:

$$d_1 = d_1 \tag{14}$$

$$d_2 = (\sqrt{2} - 1) d_1 \tag{15}$$

$$d_3 = \left(\frac{3 - 2\sqrt{2}}{3 - \sqrt{2}}\right) d_1 \tag{16}$$

where d_1 is the diameter of the principal or first construct. Higher order constructs ($n \geqslant 4$) are more difficult to derive and are also of lesser value due to their diminished size.

As we strive for maximum global performance, we will also consider any gains made through the use of multi-scale design by comparing with the special case of a volume containing only

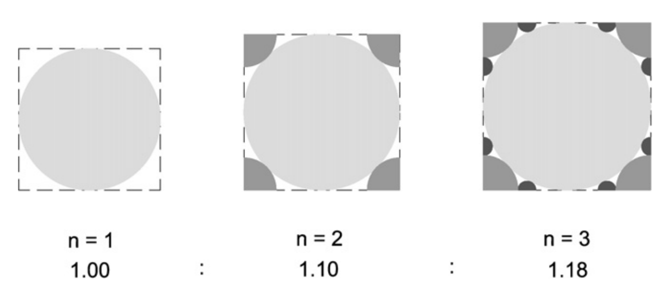

Fig. 4. A comparison of the relative size of the basic cell for each constructal design.

parallel plates. This fundamental solution was obtained by Bejan and Sciubba [8] and provides the following approximate results:

$$\frac{b_{opt}}{L} \approx 2.726 Be^{-1/4} \quad (17)$$

and

$$Q^\star \lesssim 0.6192 Be^{1/2} \quad (18)$$

It was shown by the author [5] that this is the best overall geometry when considering exact results provided in Table 1, under the constraints of fixed volume and pressure drop.

3.1. First construct ($n = 1$)

The first construct is shown in Fig. 4(a). The basic duct arrangement is a simple square packing arrangement with $N_1 \sim HW/d_1^2$. The solution for the first construct was obtained in a recent paper by the author [5]:

$$\frac{d_{1,opt}}{L} \approx 4.683 Be^{-1/4} \quad (19)$$

The maximum heat transfer rate for this arrangement was found to be of the order:

$$Q^\star \lesssim 0.5382 Be^{1/2} \quad (20)$$

3.2. Second construct ($n = 2$)

If additional tubes representing the second construct are added to the intersticial regions, as shown in Fig. 4(b), a general improvement is achieved, but the arrangement is not optimal, as the secondary tube diameter is sub-optimal. Eq. (12) allows for the coupling of the first and second contructs, which leads to an optimal solution for the pairing of the first and second constructs.

The solution for the second construct when $N_1 \sim HW/d_1^2$ and $N_2 \sim N_1$ for the basic cell, produces the following results:

$$\frac{d_{1,opt}}{L} \approx 5.152 Be^{-1/4} \quad (21)$$

The diameter of the principal construct has now increased to allow for increased performance through the addition of the second construct. Intuitively, one should expect this behavior. The maximum heat transfer rate density for the new arrangement was found to be of the order:

$$Q^\star \lesssim 0.6701 Be^{1/2} \quad (22)$$

The solution for the coupling of the first and second constructs provides for a nearly 25% increase in heat transfer rate density. Further, this approximate theoretical result exceeds the approximate theoretical result for parallel plate channels, Eq. (18).

3.3. Third construct ($n = 3$)

Repeating the procedure one more time with $N_1 \sim HW/d_1^2$, $N_2 \sim N_1$, and $N_3 = 4N_1$, for the basic cell containing the addition of the third construct, as shown in Fig. 4(c), leads to:

$$\frac{d_{1,opt}}{L} \approx 5.535 Be^{-1/4} \quad (23)$$

Once again, the principal construct (and the second) has increased in size to allow for better global performance of the structure. The maximum heat transfer rate density is now found to be of the order:

$$Q^\star \lesssim 0.7740 Be^{1/2} \quad (24)$$

The solution for the coupling of the third construct to the first and second constructs, yields a further increase in heat transfer density of approximately 15%. Overall, the heat transfer rate density increases by 44% over the case when only one construct is used. The heat transfer density using the second and third constructs, now far exceeds the theoretical value for systems containing parallel plates.

The relative changes in size of the basic cell for each of the tube layouts is shown in Fig. 4, which compares the three constructal designs. The basic cell containing the second construct is approximately 10% larger than the first construct, while the basic cell containing the second and third constructs is approximately 18% larger than the first construct. It is this freedom to morph, as constructs are added, that allow for the system's global performance to increase.

4. Exact analysis

The heat transfer rate for the three constructal designs, may be computed using an exact analytical approach for isothermal tubes. The heat transfer rate will be computed using an effectiveness-number of transfer units, *e-NTU* model for parallel flow through an isothermal system [11]:

$$Q = \dot{m} C_p (\overline{T}_s - T_i)\left[1 - \exp\left(-\frac{\bar{h} P L}{\dot{m} C_p}\right)\right] \quad (25)$$

The mass flow rate for a prescribed pressure drop is computed using the model of Muzychka and Yovanovich [10] for the apparent friction factor for hydrodynamically developing flows:

$$f_{app} Re_{\sqrt{A}} = \left[(f\,Re_{\sqrt{A}})^2 + \left(\frac{3.44}{\sqrt{z^+}}\right)^2\right]^{1/2} \quad (26)$$

where

$$z^+ = \frac{L}{\sqrt{A}\, Re_{\sqrt{A}}} = \frac{\mu L}{\dot{m}}$$

and

$$f\,Re_{\sqrt{A}} = 8\sqrt{\pi}$$

It is clear when L is fixed, the value of z^+ may also be interpreted as a form of dimensionless mass flow rate.

The heat transfer coefficient is computed using the general model of Muzychka and Yovanovich [10] for the Nusselt number for simultaneously developing flows. It is given below in a form which is valid for an isothermal tube:

$$Nu_{\sqrt{A}}(z^*) = \left[\left(\frac{2 f(Pr)}{\sqrt{z^*}}\right)^m + \left(\left\{0.614\left(\frac{f\,Re_{\sqrt{A}}}{z^*}\right)^{1/3}\right\}^5 + 3.01^5\right)^{m/5}\right]^{1/m} \quad (27)$$

where

$$z^* = \frac{L}{\sqrt{A}\, Re_{\sqrt{A}} Pr} = \frac{\mu L}{\dot{m}\, Pr}$$

and

$$f(Pr) = \frac{0.564}{[1 + (1.664 Pr^{1/6})^{9/2}]^{2/9}} \tag{28}$$

and

$$m = 2.27 + 1.65 Pr^{1/3} \tag{29}$$

The use of Eqs. (25)–(27) requires the definition of a parametric variable. The scaling law derived from the approximate intersection of asymptotes method provides such a variable [8]:

$$\delta_1 = \frac{d_1}{L} Be^{1/4} \tag{30}$$

Eq. (26) may then be written as:

$$\delta_1^4 = g_1(z^+, Pr) \tag{31}$$

since,

$$f_{app} Re_{\sqrt{A}} = \frac{2A}{P} \frac{\Delta p}{L} \frac{\sqrt{A}}{\mu \overline{U}} \tag{32}$$

while Eq. (27), may be written as:

$$Nu_{\sqrt{A}} = g_2(z^+, Pr) \tag{33}$$

Finally, Eq. (25) may be written in dimensionless form as:

$$\frac{Q^\star}{Be^{1/2}} = g_3(\delta_1, z^+, Nu_{\sqrt{A}}, Pr) \tag{34}$$

The parametric solution for a given value of Prandtl number, requires that z^+ be specified. The value of δ_1 may then be solved for using Eq. (26), next $Nu_{\sqrt{A}}$ is found, and finally, $Q^\star/Be^{1/2}$ is calculated using the list $[Pr, z^+, \delta_1, Nu_{\sqrt{A}}]$. The process is then repeated for a new value of z^+ and so forth. The resulting parametric analysis yields a plot of $Q^\star/Be^{1/2}$ versus δ_1, which then gives the optimal value of δ_1. In the case of a multi-scale design, Eqs. (25)–(27) are also written for each tube scale giving δ_i where $i = 1, \ldots, 3$, and the total heat transfer rate density taken as the sum of the three contributions. The additional equations may then be written in terms of δ_1, the principal construct, using Eqs. (14)–(16). The solution procedure now requires that the following list of variables be stated and/or solved for, in the following order: $[Pr, z_1^+, \delta_1, z_2^+, Nu_1, Nu_2, Q^\star/Be^{1/2}]$ for $n = 2$ or $[Pr, z_1^+, \delta_1, z_2^+, z_3^+, Nu_1, Nu_2, Nu_3, Q^\star/Be^{1/2}]$ for $n = 3$.

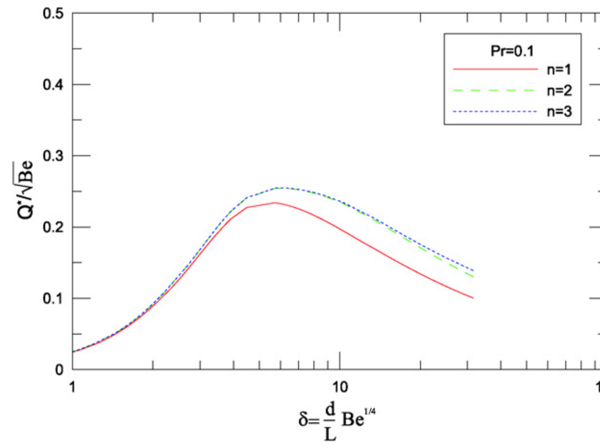

Fig. 5. Exact results for $Pr = 0.1$.

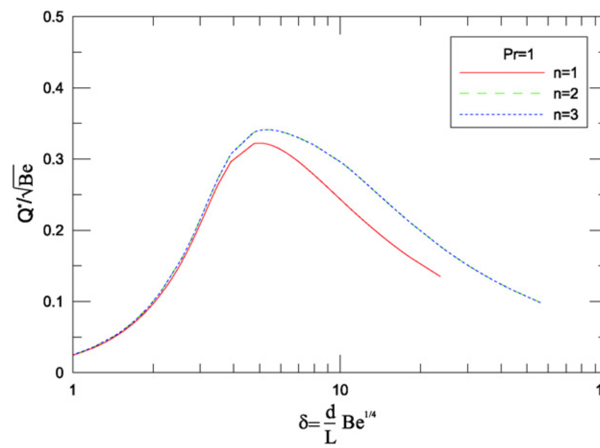

Fig. 6. Exact results for $Pr = 1$.

The results of the analysis are summarized in Table 2 and in Figs. 5–9. For $n = 1$, the case of a single construct, the results are in excellent agreement with those in Table 1 obtained by Yilmaz et al. [9]. The small differences are due to the use of different models for $f_{app} Re$ and Nu. The gains in dimensionless heat transfer rate density are significantly smaller than the approximate relationships indicated. Further, the exact analysis reveals that there is virtually no advantage to using the third construct. The theoretical gain of 15% is masked as a result of the approximate nature of the solution. Typically, the gains made in using the second construct range from 6–10%.

Table 2 also summarizes the results obtained using Eqs. (25)–(27) when the *approximate* solutions for $d_{1,opt}$ are used. Clearly,

Table 2
Exact and approximate results for each constructal level

Pr	$(n = 1)$			$(n = 2)$			$(n = 3)$			Parallel plates
	δ_1	$Q_e^\star/Be^{1/2}$	$Q_a^\star/Be^{1/2}$	δ_1	$Q_e^\star/Be^{1/2}$	$Q_a^\star/Be^{1/2}$	δ_1	$Q_e^\star/Be^{1/2}$	$Q_a^\star/Be^{1/2}$	$Q_e^\star/Be^{1/2}$
0.1	5.718	0.2339	0.2304	5.937	0.2543	0.2511	5.938	0.2548	0.2539	0.3541
1	4.912	0.3223	0.3209	5.301	0.3412	0.3410	5.301	0.3416	0.3414	0.4905
10	5.165	0.3588	0.3544	5.747	0.3802	0.3779	5.747	0.3806	0.3805	0.5230
100	5.351	0.3669	0.3601	6.085	0.3906	0.3853	6.085	0.3911	0.3894	0.5250
1000	5.344	0.3679	0.3607	6.072	0.3921	0.3862	6.072	0.3926	0.3905	0.5223

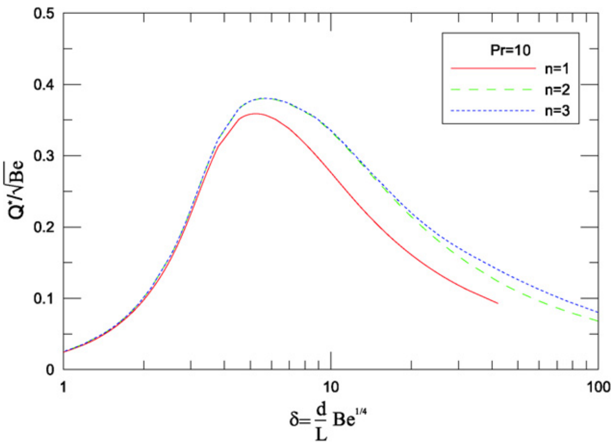

Fig. 7. Exact results for $Pr = 10$.

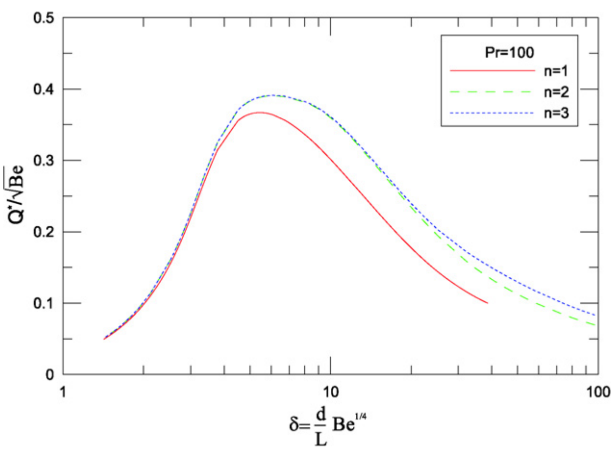

Fig. 8. Exact results for $Pr = 100$.

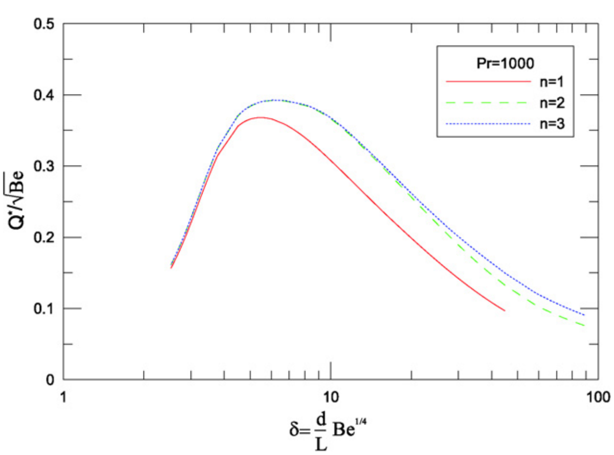

Fig. 9. Exact results for $Pr = 1000$.

near exact solutions are obtained using the *approximate* solution for the geometry with fundamental heat transfer theory.

Finally, it should be noted that although gains were made using the idea of multiple scales, the results still do not equal or exceed those of the parallel plate channel for the same Prandtl number. The parallel plate structure still provides 33–43% greater heat transfer rate density, due to the smaller plate spacing and more efficient packing of surface area. If surface area is also constrained, then the problem becomes one of optimal distribution of flow resistances. In this case both systems, that is, one with channels and the other with tubes, will have approximately the same overall heat transfer density, with one marginally performing better than the other.

We conclude with an illustrative example which demonstrates a number of fundamental issues. Consider the design of a water cooled chip cooler of nominal dimensions $W = 50.8$ mm, $H = 25.4$ mm, $L = 50.8$ mm, $\Delta p = 1000$ Pa, and $\overline{T}_s - T_i = 25$ K. The properties may be taken as: $C_p = 4176\ \mathrm{J\,kg^{-1}\,K^{-1}}$, $\rho = 997\ \mathrm{kg\,m^{-3}}$, $k_f = 0.613\ \mathrm{W\,m^{-1}\,K^{-1}}$, $\alpha = 0.1471\mathrm{e}{-6}\ \mathrm{m^2\,s^{-1}}$, $\nu = 0.8576\mathrm{e}{-6}\ \mathrm{m^2\,s^{-1}}$, and $Pr = 5.83$. Using Eqs. (19) and (25)–(27), we may easily show that for a system using only first constructs, $d_{1,opt} = 0.629$ mm and a heat transfer rate of $Q = 19\,753$ W result. Next, if we now assume that the principal diameter remains the same but we choose to fill the intersticial regions with a second but sub-optimal construct, the heat transfer rate becomes $Q = 20\,635$ W. However, if we now use the new principal diameter for the case where two constructs are coupled, Eq. (21), one now obtains $d_{1,opt} = 0.692$ mm and $Q = 21\,116$ W. The difference between the first and second constructs is approximately 7%. It is now clear that the enlargement of the principal construct does allow for maximal heat transfer density when a second construct is used. It may also be shown that further changes in $d_{1,opt}$ lead to sub-optimal performance. Finally, it should be pointed out that in this case, the thermal entrance length for the principal construct is $L/d\,Re_d Pr = 0.049$, and $L/d\,Re_d Pr = 1.55$ for the second construct. The latter gives rise to local Nusselt numbers which are nearly at fully developed flow values. Thus, the third construct which contributes very little, represents thermally fully developed flow, which should be avoided in practical design applications. The principal construct always yields a system design which is of the same order as the thermal entrance length.

5. Summary and conclusions

A constructal multi-scale design of a micro-tube heat sink/heat exchanger was considered. It was shown that through the use of intersticial tubes, maximum heat transfer rates for arrays of circular tubes were increased, but did not surpass rates for arrays of parallel plates. Approximate results were obtained using the intersection of asymptotes method. These approximate solutions were compared with exact results using semi-analytical relationships for fluid friction and heat transfer in tubes. In general, through the use of multi-scale design techniques, greater performance of heat sink/heat exchanger core structures can be obtained versus conventional design approaches. The method is robust and may be applied to systems with different tube layouts from those considered, assuming that the distribution of tubes (or scales) is known. Finally, it was demonstrated that using the approximate solution for internal geometry, when combined with fundamental heat transfer theory for heat exchangers, provided excellent results for the heat transfer rate density.

Acknowledgements

The author acknowledges the financial support of the Natural Sciences and Engineering Research Council of Canada (NSERC) through the discovery research grants program. The author also acknowledges the assistance of Kelly Boone and Zhipeng Duan for preparation of the figures, and Adrian Bejan for some insightful comments.

References

[1] A. Bejan, Designed porous media: Maximal heat transfer density at decreasing length scales, International Journal of Heat and Mass Transfer 47 (2004) 3073–3083.
[2] A. Bejan, I. Dincer, S. Lorente, A.F. Miguel, A.H. Reis, Porous and Complex Flow Structures in Modern Technologies, Springer, New York, 2004.
[3] A. Bejan, Convection Heat Transfer, Wiley, New York, 2004, pp. 136–141.
[4] A. Bejan, Shape and Structure: From Engineering to Nature, Cambridge University Press, Cambridge, UK, 2000, pp. 35–37.
[5] Y. Muzychka, Constructal design of forced convection cooled microchannel heat sinks and heat exchangers, International Journal of Heat and Mass Transfer 48 (2005) 3119–3127.
[6] A. Bejan, Y. Fautrelle, Constructal multi-scale structure for maximal heat transfer density, Acta Mechanica 163 (2003) 39–49.
[7] T. Bello-Ochende, A. Bejan, Maximal heat transfer density: Plates with multiple lengths in forced convection, International Journal of Thermal Sciences 43 (2004) 1181–1186.
[8] A. Bejan, E. Sciubba, The optimal spacing of parallel plates cooled by forced convection, International Journal of Heat and Mass Transfer 35 (1992) 3259–3264.
[9] A. Yilmaz, O. Buyukalaca, T. Yilmaz, Optimum shape and dimensions of ducts for convective heat transfer in laminar flow at constant wall temperature, International Journal of Heat and Mass Transfer 43 (2000) 767–775.
[10] Y.S. Muzychka, M.M. Yovanovich, Laminar forced convection heat transfer in combined entrance region of non-circular ducts, Journal of Heat Transfer 126 (2004) 54–61.
[11] R.K. Shah, D. Sekulic, Fundamentals of Heat Exchanger Design, Wiley, New York, 2003, pp. 473–508.